

Dynamic Mixture of Progressive Parameter-Efficient Expert Library for Lifelong Robot Learning

Yuheng Lei^{1,2}, Sitong Mao³, Shunbo Zhou³, Hongyuan Zhang^{1,2}, Xuelong Li², Ping Luo^{1,4}

¹ The University of Hong Kong

² Institute of Artificial Intelligence (TeleAI), China Telecom

³ Huawei Cloud Computing Technologies

⁴ HKU Shanghai Intelligent Computing Research Center

leiylh@connect.hku.hk, pluo@cs.hku.hk

Abstract

A generalist agent must continuously learn and adapt throughout its lifetime, achieving efficient forward transfer while minimizing catastrophic forgetting. Previous work within the dominant pretrain-then-finetune paradigm has explored parameter-efficient fine-tuning for single-task adaptation, effectively steering a frozen pre-trained model with a small number of parameters. However, in the context of lifelong learning, these methods rely on the impractical assumption of a test-time task identifier and restrict knowledge sharing among isolated adapters. To address these limitations, we propose Dynamic Mixture of Progressive Parameter-Efficient Expert Library (DMPEL) for lifelong robot learning. DMPEL progressively learn a low-rank expert library and employs a lightweight router to dynamically combine experts into an end-to-end policy, facilitating flexible behavior during lifelong adaptation. Moreover, by leveraging the modular structure of the fine-tuned parameters, we introduce coefficient replay to guide the router in accurately retrieving frozen experts for previously encountered tasks, thereby mitigating catastrophic forgetting. This method is significantly more storage- and computationally-efficient than applying demonstration replay to the entire policy. Extensive experiments on the lifelong manipulation benchmark LIBERO demonstrate that our framework outperforms state-of-the-art lifelong learning methods in success rates across continual adaptation, while utilizing minimal trainable parameters and storage.

1 Introduction

A generalist agent should have the capability to learn and adapt continuously throughout its lifetime, usually termed as *lifelong learning* [1–6]. The longstanding challenges are enabling *forward transfer* (i.e., leveraging knowledge from previous tasks to quickly adapt to new ones) and avoiding *catastrophic forgetting* (i.e., retaining previously acquired knowledge when learning new tasks) under *limited computational and memory capacity*.

Due to the notorious sample inefficiency of the traditional *tabula rasa* approach in robotics, researchers have recently explored the *pretrain-then-finetune* paradigm [7–12] that originates from the vision and language domains [13–20]. Specifically, this paradigm first pretrain a policy, often referred to as a *vision-language-action* (VLA) model, on large-scale datasets, and then fine-tune it for various downstream tasks. However, in the context of lifelong learning, naively applying full fine-tuning to sequentially arriving robotic tasks can result in severe forgetting and suboptimal performance, failing to meet our requirements. As depicted in Figure 1, prior work in lifelong robot learning can be broadly classified into three distinct approaches. *Replay* methods [8, 21–25] retain previous data (e.g., vision-language web data, robot pretraining data, and data from seen tasks) and mix it with in-domain

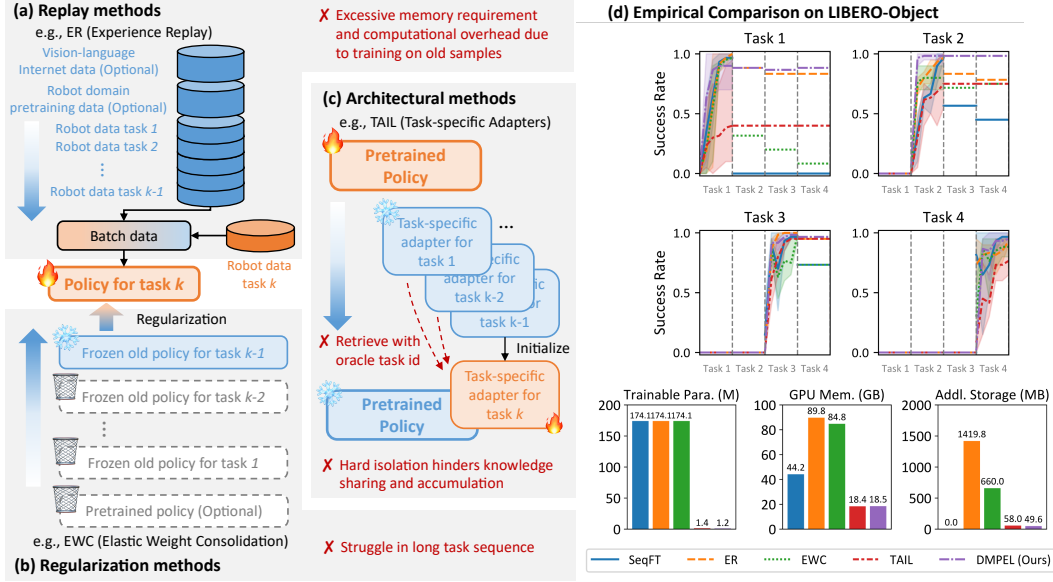


Figure 1: Existing lifelong learning methods: (a) Replay methods; (b) Regularization methods; (c) Architectural methods; (d) Performance on LIBERO-Object. TAIL with LoRA utilizes significantly fewer resources than ER/EWC with FFT and exhibits no forgetting when provided with a task identifier, but demonstrates lower forward transfer. In contrast, DMPEL leverages a low-rank expert library and coefficient replay (CR=5%) to achieve better forward transfer and near-zero forgetting.

data during training on new tasks. These methods leads to generalizable policies, but also necessitates huge storage space and computational overhead for retaining old samples. *Regularization* methods [26–28] balance between new and old tasks by restricting the update of parameters. For example, EWC [27] require an entire copy of frozen model from the previous task and entail substantial computation in estimating the importance of parameters. In addition, they usually struggle in long task sequence due to plasticity-stability dilemma.

In contrast, *architectural methods* [29–31] address catastrophic forgetting by explicitly learning task-specific parameters. The widely adopted *parameter-efficient fine-tuning* (PEFT) techniques [32, 33], such as adapters [34, 35], low-rank adaptation (LoRA) [36], and prompt tuning [37–39], have proven highly effective for steering frozen foundation models by integrating small, learnable modules in single-task adaptation. In the lifelong learning setting, a practical solution, as exemplified by TAIL [40], involves initializing and training task-specific adapters for each task, subsequently freezing them, and retrieving the appropriate adapter based on the oracle task index. Such method allows efficient adaptation with only a small amount of task-specific parameters, but also exhibits certain limitations. First, assuming test-time task identity is known and retrieving adapter in a hard-coded way could be impractical in real scenarios. Second, failing to effectively share knowledge across isolated adapters result in poor forward transfer. Some prior arts construct a shared adapter pool and enable automatic timestep-level retrieval by, for example, performing query-key matching to select the one with highest similarity from a pool of adapters [41], or using multifaceted prototypes to represent the cluster center in the state space for each adapter [42], but usually suffer from inaccurate retrieval and suboptimal performance.

In this paper, we introduce Dynamic Mixture of Progressive Parameter-Efficient Expert Library (DMPEL) to overcome these challenges in lifelong robot learning. DMPEL incrementally builds a library of low-rank experts and uses a lightweight router to dynamically assemble these experts into a unified policy, enabling the agent to adapt flexibly throughout continual adaptation. By exploiting the modularity of fine-tuned parameters, DMPEL incorporates coefficient replay at the router, enabling the policy to accurately integrate experts for all previously seen tasks and thereby effectively preventing catastrophic forgetting. This approach is significantly more efficient in terms of storage and computation than replaying expert demonstrations for the entire policy. Through extensive evaluations on the LIBERO lifelong manipulation benchmark [43], we show that our method achieves higher forward transfer and lower catastrophic forgetting than existing baselines while requiring minimal trainable parameters and storage. Code is publicly released for reproducibility.

2 Related Work

Foundation Models for Robotics. The traditional *tabula rasa* paradigm in robotics is widely criticized for its sample inefficiency, prompting researchers to explore the use of foundation models to improve downstream task transfer [44, 45]. One prominent direction involves transferring general visual representations: some studies directly employ foundation models from other domains, such as CLIP [15], SAM [18], and DINOv2 [14], as vision encoders [46, 47], while others pretrain visual representations using self-supervised learning [16, 17] on egocentric video datasets like R3M [48], MVP [49], and VC-1 [50]. Another emerging line of research focuses on pretraining large-scale policies on diverse robotic tasks to capture generalizable behavior priors, for example, RT-1 [7], RT-2 [8], Gato [9], Octo [10], OpenVLA [11], and π_0 [12]. However, when adapting these models to downstream tasks, most approaches either rely on the frozen pretrained model (i.e., zero-shot transfer) or require costly full fine-tuning. Some prior work has explored parameter-efficient fine-tuning (PEFT) by integrating task-specific modules into the pretrained vision encoder [51–53] or temporal transformer [54–56]. Despite these advancements, the majority of these methods focus on single-stage adaptation, whereas our approach targets lifelong adaptation to a sequence of new tasks.

Lifelong Learning with PEFT. Compared to full fine-tuning, PEFT optimizes only a small amount of inserted parameters and keeps the rest untouched, greatly reducing the storage cost of tuned parameters and mitigating the risk of overfitting in low-data regimes [32]. Notably, PEFT techniques share conceptual similarities with architectural methods in lifelong learning. Most studies on lifelong learning with PEFT predominantly utilize prompt-based tuning [37, 39] to adapt frozen pretrained model for tasks such as image classification (e.g., L2P [57], DualPrompt [58], CODA-Prompt [59], and DAP [60]) and text classification (e.g., EPI [61], and Progressive Prompts [62]). Current research primarily investigates strategies for dynamically selecting or generating instance-specific prompts [63]. Recognizing the representational limitations of prompt tuning, subsequent studies have extended to more powerful PEFT techniques, including LAE [64], HiDe-PET [65]. Despite the demonstrated success of PEFT-based lifelong learning in classification tasks, its application remains largely unexplored in robotics. A few pioneering works employ LoRA [36] to store task-specific knowledge, yet diverge in their retrieval mechanisms: TAIL [40] relies on oracle task identifier, L2M [41] implements query-key matching between the current context (the state embedding from the frozen pretrained model) and learnable keys, while IsCiL [42] establishes multifaceted prototypes through K-means clustering in the state space, with input states retrieving the closest LoRA parameters based on proximity. Our method incrementally constructs a parameter-efficient expert library and learns a lightweight router to dynamically retrieve and combine these experts.

Mixture of Experts (MoE) and Model Fusion. The Mixture of Experts (MoE) approach, which involves training multiple specialized models for specific subtasks, has gained significant attention [66–68]. A key method for combining these experts is parameter ensemble, supported by the linear mode connectivity phenomenon, which shows models converging to a single low-loss basin [69]. Task Arithmetic [70] introduces *task vectors*, representing the difference between fine-tuned and pretrained models, enhancing multi-task model performance when merged. Follow-up work [71, 72] improves this by learning input-conditioned layer-wise fusion coefficients, increasing flexibility and performance. Model fusion techniques also apply to PEFT, where previously learned adapters are reused for efficient task adaptation [73–76], including LoRAHub [77] and AdapterFusion [78]. In image generation, merging separate LoRAs facilitates joint style and content generation [79–81]. In robotics, models like MELA [82], MoE-LoCo [83], MORE [84], and SDP [85] create versatile, adaptive behaviors for multiple tasks by fusing expert sets. Our method aims to enhance forward transfer in lifelong robot learning by flexibly fusing previously learned low-rank experts for each sub-module in the policy. Besides, we exploit the modularized design by replaying coefficient on the router to mitigate catastrophic forgetting.

3 Problem Formulation

3.1 Lifelong Robot Learning

In this paper, we aim to solve language-conditioned vision-based robot manipulation task, which can be formulated as a finite-horizon Markov Decision Process (MDP) $\mathcal{M} = (\mathcal{S}, \mathcal{A}, \mathcal{P}, \mathcal{H}, d_0, l)$, where

\mathcal{S} and \mathcal{A} is the state space and action space of robot, $\mathcal{P} : \mathcal{S} \times \mathcal{A} \rightarrow \mathcal{S}$ is the transition dynamics, \mathcal{H} is the episode length, and each task $\mathcal{T} \triangleq (d_0, l)$ is defined by the initial state distribution d_0 and the goal predicate in the form of language instruction $l : \mathcal{S} \rightarrow \{0, 1\}$. The ultimate objective of robot learning is to search for a policy π that maximizes the expected success rate in reaching the goal: $\max_{\pi} J(\pi) = \mathbb{E}_{s_t, a_t \sim \pi, d_0} \left[\sum_{t=1}^{\mathcal{H}} l(s_t) \right]$.

Due to the significant challenge of sparse reward in robot manipulation, we consider a more practical lifelong imitation learning setting [43, 40], where a robot sequentially learns over a stream of tasks $\{\mathcal{T}^1, \dots, \mathcal{T}^K\}$ given an expert demonstration dataset $\mathcal{D}^k = \{\tau_n^k\}_{n=1}^N$ for each task $\mathcal{T}^k = (d_0^k, l^k)$, $1 \leq k \leq K$. Each expert trajectory τ_n^k can be represented as $(o_0, a_0, \dots, o_{\mathcal{H}})$, in which observation o_t at each step t includes RGB images and proprioceptive states. Following common practice in partially observable MDPs, we approximate the current state s_t by stacking prior observations, i.e., $s_t = o_{\leq t} = (o_0, \dots, o_t)$. We perform behavior cloning [86] to learn a stochastic policy π_{θ} by minimizing the negative log-likelihood loss L :

$$\min_{\theta} L(\theta) = -\mathbb{E}_{\tau_n^k \sim \mathcal{D}^k} \left[\sum_{t=0}^{\mathcal{H}-1} \log \pi_{\theta}(a_t | o_{\leq t}, l^k) \right]. \quad (1)$$

3.2 Evaluation Metrics

We use three metrics to evaluate the performance of lifelong robot learning [43, 87]: forward transfer (FWT), negative backward transfer (NBT), area under the success rate curve (AUC). Formally, we evaluate the policy on current task \mathcal{T}^k when reaching a checkpoint $c \in \mathcal{C}$ (i.e., every multiple epochs of training) and we denote the success rate during evaluation as $s_{k,k,c}$. When the training on current task is completed, we find the earliest checkpoint c_k^* that achieves the best performance and mark it as the final success rate $s_{k,k}$, i.e., $s_{k,k} = s_{k,k,c_k^*} = \max_{c \in \mathcal{C}} s_{k,k,c}$. We only keep the best checkpoint for future training and evaluation as if the agent stops learning after c_k^* , i.e., for all $c \geq c_k^*$, $s_{k,k,c} = s_{k,k}$. This checkpoint c_k^* will be further evaluated on previous tasks $\mathcal{T}^j, j \leq k$, where the success rate is denoted as $s_{k,j}$. Then we can define the three metrics as:

$$\text{FWT} = \frac{1}{K} \sum_{k=1}^K \left[\frac{1}{|\mathcal{C}|} \sum_{c \in \mathcal{C}} s_{k,k,c} \right], \quad (2)$$

$$\text{NBT} = \frac{1}{K} \sum_{k=1}^K \left[\frac{1}{K-k} \sum_{l=k+1}^K (s_{k,k} - s_{l,k}) \right], \quad (3)$$

$$\text{AUC} = \frac{1}{K} \sum_{k=1}^K \left[\frac{1}{K-k+1} \left(\frac{1}{|\mathcal{C}|} \sum_{c \in \mathcal{C}} s_{k,k,c} + \sum_{l=k+1}^K s_{l,k} \right) \right]. \quad (4)$$

Intuitively, higher FWT indicates faster adaptation to new tasks, lower NBT indicates less catastrophic forgetting on old tasks, and higher AUC demonstrates an overall better performance across tasks and a good balance between FWT and NBT.

4 Proposed Method

4.1 Base Policy Architecture

We use an autoregressive policy [11, 88] similar to the one used in the LIBERO benchmark [40, 43] and focus on developing better lifelong learning algorithms. The policy consists of vision, text, and state encoders, an input modality fusion module, a temporal transformer, and an action head.

Vision, text, and state encoders. The policy input is the historical observations (o_{t-T}, \dots, o_t) and the language instruction $l = \{l_i\}_{i=1}^L$, where T is the context length and L is the sentence length. The observation at each step $o_t = (I_t^1, \dots, I_t^{N_c}, p_t)$ includes RGB images $I_t^{n_c}, 1 \leq n_c \leq N_c$ from N_c different cameras and low-dimensional proprioceptive states p_t . In experiments, we use images from two cameras, the agent-view image and the eye-in-hand image. We employ the pretrained CLIP ViT-B/16 model [15] to serve as the vision encoder \mathcal{E}_I and the text encoder \mathcal{E}_L . For the joint states

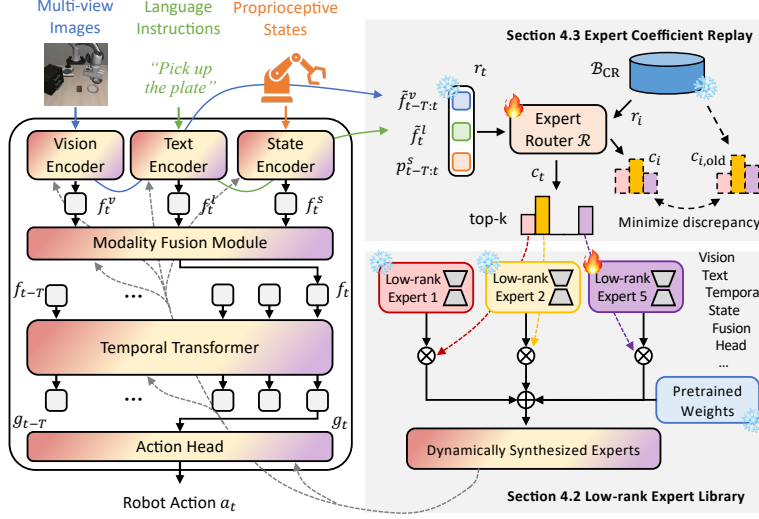


Figure 2: Overview of the proposed method DMPEL.

and gripper states, we learn separate linear projection layers \mathcal{E}_P to project the low-dimensional states to proprioceptive embeddings. In summary, at each timestep, we obtain image embeddings f_t^v , text embeddings f_t^l , and proprioceptive embeddings f_t^s .

Modality fusion. We utilize a feature-wise linear modulation (FiLM) [89] to fuse language embeddings with the image and state embeddings. Generally, given the original feature x , the conditional input z , and the fusion network f_{FiLM} , we can obtain the modulated feature $x' = \gamma \odot x + \beta$ where $\gamma, \beta = f_{\text{FiLM}}(z)$. In our case, the conditional input z refers to the language embedding f_t^l , γ and β are scaling and shifting vectors having the same size as x , and \odot refers to element-wise multiplication.

Temporal transformer and action head. The causal temporal transformer backbone processes a sequence of multi-modal embeddings to produce a latent vector g_t at each decision-making timestep. We employ a Gaussian Mixture Model (GMM)-based output head to compute the multi-modal distribution of manipulation actions [40, 43]. During training, we optimize the negative log-likelihood loss between the action distribution and the ground truth action. At inference time, the robot executes the policy by using the mean of the Gaussian distribution with the highest density for end effectors.

4.2 Low-rank Expert Library

Following the pretrain-then-finetune paradigm, we pretrain the policy on a large-scale robotic dataset and freeze it during the lifelong adaptation to unseen downstream tasks.

Low-Rank Adaptation (LoRA) [36]. A representative parameter-efficient fine-tuning (PEFT) method that introduces learnable low-rank matrices $\mathbf{A} \in \mathbb{R}^{d_{\text{in}} \times r}$, $\mathbf{B} \in \mathbb{R}^{r \times d_{\text{out}}}$ and integrate in parallel with the frozen weight matrix $\mathbf{W}_0 \in \mathbb{R}^{d_{\text{in}} \times d_{\text{out}}}$ through addition, i.e., $\mathbf{W}_0 + \mathbf{A}\mathbf{B}$. By leveraging the low-rank decomposition $r \ll \min\{d_{\text{in}}, d_{\text{out}}\}$, LoRA substantially reduces the number of trainable parameters.

Existing PEFT methods learn a task-specific low-rank adapter $\Delta\mathbf{W}_k = \mathbf{A}_k\mathbf{B}_k$ for each task \mathcal{T}_k in lifelong robot learning [40, 41]. Such design requires task identifier during inference, lacks flexibility due to fixed capacity, and also hinders knowledge sharing across tasks. Prior arts in vision and language domain, e.g., LoRAHub [77] and SD-LORA [90], use a task-wise learnable weight vector to combine existing low-rank experts for better performance on the new task. A key insight is that these low-rank experts captures complementary knowledge from a variety of specific tasks and can be leveraged to solve a new task. However, lifelong learning in robotic domain could be even more challenging. First, compared to image or text classification [1, 3, 5] that requires only single forward inference, robotic manipulation is a sequential decision-making process with long horizon. Besides, robot learning requires a mixed types of knowledge, for example, visual concepts, textual task goals,

different spatial relationships, and successful adaptation to a new task requires a combination of adaptation in each sub-modules.

Following this motivation, we propose to learn a progressive low-rank expert library on top of the pretrained policy and dynamically reuse low-rank experts from prior tasks $j \leq k - 1$ to facilitate efficient forward transfer to new task \mathcal{T}_k . We equip each chosen pretrained linear layer $\mathcal{F} = \{\mathbf{W}_0, \mathbf{b}_0\}$ with a low-rank expert library $\mathcal{L} = \{\mathbf{A}_j, \mathbf{B}_j, \mathbf{b}_j\}_{j=1}^k$ and use a global lightweight router \mathcal{R} to dynamically integrate pretrained and task-specific knowledge based on the current context, providing a more flexible solution for adaptation.

Specifically, the router $\mathcal{R} : \mathbb{R}^{d_r} \rightarrow \mathbb{R}^{6 \times k}$ is implemented as a multi-layer perceptron (MLP) to obtain the dynamic coefficient for each low-rank expert. The router input $\mathbf{r}_t = [f_{t-T:t}^v, f_t^l, p_{t-T:t}] \in \mathbb{R}^{d_r}$, where $\cdot_{t-T:t}$ indicates mean pooling over the T -step context window. This aggregated representation contains information streams from the visual embeddings, the task instruction embeddings, and also the low-dimensional proprioceptive states, and hence comprehensively encodes the current context. Then we can dynamically obtain the expert coefficient:

$$\mathbf{c}_t = [\mathbf{c}_t^v; \mathbf{c}_t^l; \mathbf{c}_t^s; \mathbf{c}_t^f; \mathbf{c}_t^t; \mathbf{c}_t^h] = \text{top-k}(\mathcal{R}(\mathbf{r}_t), \delta), \quad \mathbf{c}_t = [c_{1,t}, c_{2,t}, \dots, c_{k,t}] \in \mathbb{R}^k. \quad (5)$$

Note that the output $\mathbf{c}_t \in \mathbb{R}^{6 \times k}$ is divided into six distinct coefficient vectors, each assigned to a specific sub-module in the policy: \mathbf{c}_t^v for vision encoder, \mathbf{c}_t^l for text encoder, \mathbf{c}_t^s for state encoder, \mathbf{c}_t^f for modality fusion module, \mathbf{c}_t^t for temporal transformer, and \mathbf{c}_t^h for action head. This design allows each sub-module to use a different coefficient vector to integrate knowledge, providing larger flexibility in adaptation. The $\text{top-k}(\cdot, \delta)$ operator retains only the top- δ entries of the input vector at their original values, while setting all other coefficients to zero. This ensures efficient utilization of experts by reducing computational overhead while maintaining flexibility for adaptation. Finally, the input-conditioned linear layer $\{\tilde{\mathbf{W}}, \tilde{\mathbf{b}}\}$ is the dynamic mixture of the pretrained weight \mathcal{F} and the low-rank experts from the library \mathcal{L} :

$$\mathbf{y} = \tilde{\mathbf{W}}\mathbf{x} + \tilde{\mathbf{b}} = \underbrace{\mathbf{W}_0\mathbf{x} + \mathbf{b}_0}_{\text{pretrained}} + \underbrace{\sum_{j=1}^k c_{j,t} \mathbf{A}_j \sum_{j=1}^k c_{j,t} \mathbf{B}_j \mathbf{x} + \sum_{j=1}^k c_{j,t} \mathbf{b}_j}_{\text{fine-tuned}}. \quad (6)$$

Upon the completion of task \mathcal{T}_k , we freeze all low-rank experts in the library as acquired knowledge and initialize new learnable expert for task \mathcal{T}_{k+1} . In order to reduce the interference between tasks, we employ the Gram-Schmidt orthogonalization method on \mathbf{A}_{k+1} [59, 91], while other elements \mathbf{B}_{k+1} and \mathbf{b}_{k+1} are simply zero-initialized.

4.3 Expert Coefficient Replay

To mitigate catastrophic forgetting, we freeze the learned low-rank expert module after each task's completion for future retrieval. However, since the router is continuously updated on sequentially arriving tasks, incorrect integration of the expert, i.e., the expert coefficients are inaccurate, may lead to severe policy distortion and suboptimal performance.

Inspired by replay methods [22, 24, 76], we propose an expert coefficient replay mechanism specifically designed for the lightweight router. The implementation involves two phases: During task finalization, we archive a subset of the router's input-output pairs, i.e., the context embedding \mathbf{r} and the coefficient vector \mathbf{c} , in a dedicated buffer \mathcal{B}_{CR} . When adapting to new tasks, the core idea is to enforce consistency by requiring the router to generate coefficients that closely match the stored historical coefficients given the same context. This is achieved through minimizing a mean squared error (MSE) objective:

$$L_{\text{CR}}(\mathcal{R}) = \mathbb{E}_{(\mathbf{r}_i, \mathbf{c}_{i,\text{old}}) \sim \mathcal{B}_{\text{CR}}} \frac{1}{2} (\mathcal{R}(\mathbf{r}_i) - \mathbf{c}_{i,\text{old}})^2. \quad (7)$$

Compared with conventional expert demonstration replay that requires computation through the entire policy, our coefficient replay strategy demonstrates superior efficiency by focusing exclusively on the lightweight router and its inputs and outputs, yielding substantial reductions in both computational overhead and storage requirements.

5 Experiments

5.1 Experimental Setup

Benchmark. We conduct evaluations in LIBERO [43], a lifelong learning benchmark on robot manipulation tasks. The robot in the benchmark is situated in a tabletop environment and equipped with a 6-DOF arm and a parallel gripper. We use four lifelong learning task suites: Goal, Spatial, Object, and Long. Each suite consists of 10 robotic manipulation tasks designed to investigate the transfer of knowledge related to task goals, spatial information, and various objects. Details can be found in Appendix A.3. The benchmark also includes LIBERO-90, a collection of 90 short-horizon diverse tasks that serves as a pretraining dataset for downstream transfer.

Baselines. We consider a naive sequential fine-tuning baseline, three representative lifelong learning methods that involve tuning the entire policy, and several state-of-the-art LoRA-based methods:

- Sequential Fine-tuning (SeqFT) [43]: Naively perform full fine-tuning (FFT) or use frozen pretrained feature (FPF), i.e., freeze the spatial encoders and fine-tune the rest, on sequentially arriving robot learning tasks.
- Experience Replay (ER) [22], a *replay* method that maintains a memory buffer with samples from previous tasks. We store a subset of data after each task and uniformly sample a fixed number of replay data from the buffer along with new task data during training.
- Elastic Weight Consolidation (EWC) [27], a *regularization* method that uses the Fisher Information Matrix (FIM) to quantify the importance of each parameter and adds a regularization term to the learning objective to constrain network updates.
- PackNet [30], an *architectural* method that first trains and prunes the network to retain a fixed proportion of the most important parameters. The selected parameters are then fine-tuned and frozen to prevent forgetting.
- Lifelong knowledge Transfer Using Skills (LOTUS) [92] involves two stages: extracting temporal segment features by leveraging frozen foundation models for skill discovery, and hierarchical imitation learning with the meta-controller and a growing skill library.
- Task-specific Adapters for Imitation Learning (TAIL) [40] introduces separate LoRAs into the spatial encoder and temporal decoder for each new task. The fusion module, state encoder, and action head are also full fine-tuned and stored as task-specific adapters. TAIL requires an oracle task identifier to retrieve the corresponding adapters during inference. In order to align with other methods, we also provide the result of SeqFT (LoRA), which fine-tunes LoRA parameters sequentially.
- Learning to Modulate (L2M) [41] maintains a learnable modulation pool with keys and associated modulators. The embedded history of state tokens serves as the query vector for query-key matching, which finally steers the pretrained policy’s behavior. We follow the original paper to use a frozen fusion module and action head, and insert LoRA pools in the CLIP encoders and the temporal transformer backbone.
- Incremental Learning of Retrievable Skills for Continual Imitation Learning (IsCiL) [42] establishes multifaceted prototypes through K-means clustering in the state space, where proper LoRA-based skills is retrieved upon current input state. We define the task-specific skill the same as in TAIL [40], i.e., LoRA matrices for transformer, the fusion module, the state encoder, and the action head.

Implementation Details. We utilize the open-source CLIP ViT/B-16 model [15] as vision and text encoders, while all other components of the policy is learned from robot demonstrations. We use a six-layer temporal transformer, using the same embedding size as the CLIP model $d = 768$. The LoRA rank is set to 8 for CLIP encoders and 16 for others, the same as in [40]. We pretrain the base policy on the LIBERO-90 dataset and use it as the starting point of lifelong learning. During adaptation, we learn 10 epochs on each arriving task and evaluate every 2 epochs, using a batch size of 32 and AdamW optimizer with a learning rate of $1e-4$. We perform expert coefficient replay for 10 epochs after each task. As for the expert router, we employ a scaled sigmoid output activation to restrict the coefficient in $[0, 2]$ and use a top-3 strategy to select useful experts. All results are averaged over three random seeds. More details can be found in Appendix A.

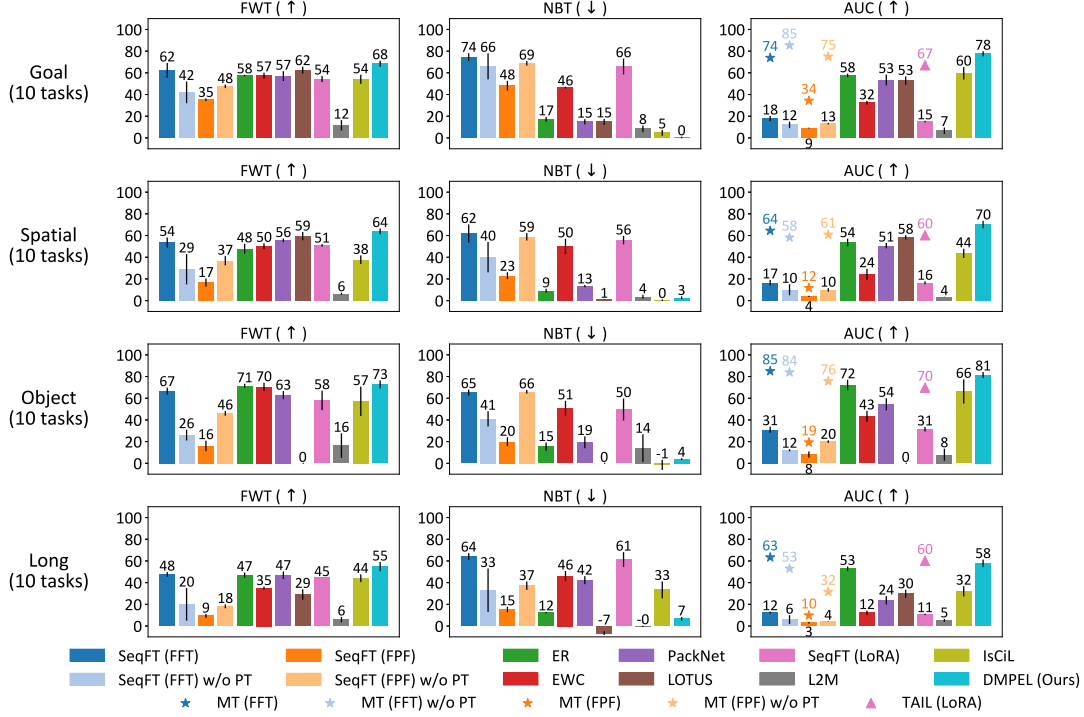


Figure 4: Performance of different lifelong robot learning methods on the LIBERO benchmark.

5.2 Results and Analysis

Main Results. Figure 3 presents the performance of the pretrained policy on both the original training tasks and zero-shot on unseen tasks, while Figure 4 summarizes three key metrics mentioned in Section 3.2 across all evaluated lifelong learning methods. Pretraining with FFT improves downstream transfer as expected, but still results in poor zero-shot performance, highlighting the need for more effective adaptation strategies. Besides, using frozen CLIP features is inefficient for robotic manipulation and performs even worse when pretraining is applied, likely due to overfitting in other sub-modules. Notably, there is a huge gap between multi-task (MT) and sequential fine-tuning (SeqFT). Among the full fine-tuning methods, ER achieves the best results, but this comes at the cost of storing and replaying large amounts of previous data (see Figure 1). LOTUS fails on the Object suite with the same code as on other suites, indicating poor robustness. Existing LoRA-based methods show lower forward transfer compared to FFT approaches, while DMPeL improves forward transfer by using dynamically synthesized experts, which reuse previous knowledge in a flexible way. Furthermore, our expert coefficient replay mechanism is highly effective in mitigating catastrophic forgetting, achieving near-zero NBT across all benchmarks without using oracle task identifiers. Conversely, L2M demonstrates weak forward transfer, likely due to its frozen action head. Although IsCiL reduces forgetting on simpler suites, it struggles with long-horizon tasks, presumably because of its fixed context encoding mechanism. In summary, DMPeL achieves efficient forward transfer and low catastrophic forgetting during lifelong learning, with only 1.2M trainable parameters (less than 0.7% of the policy) and minimal storage overhead.

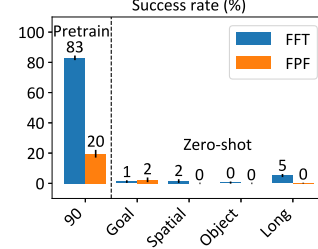


Figure 3: Performance of the pretrained policy on LIBERO

Ablation Studies. Figure 5a examines the effects of various algorithm settings. Utilizing the top-3 experts yields better performance compared to using only the top-1 expert or merging all experts. Additionally, orthogonal initialization of new experts helps to reduce interference. Besides, directly synthesizing policy parameters and assigning distinct coefficients to different submodules allows for more flexible and effective integration of knowledge. Figure 5b illustrates the impact of the coefficient

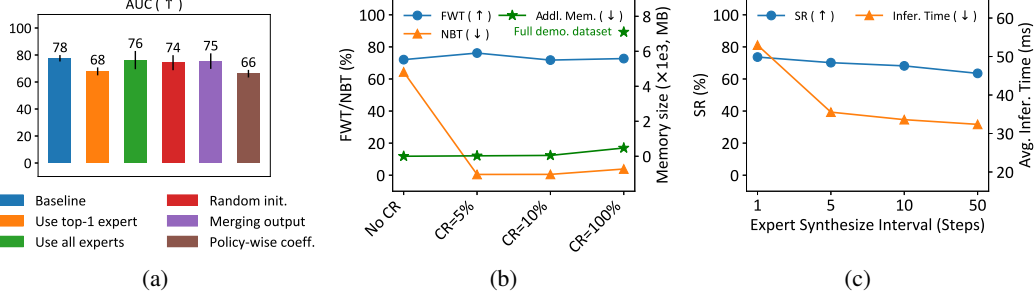


Figure 5: Ablation studies. (a) Different algorithm settings on LIBERO-Goal (b) Different coefficient replay ratios on LIBERO-Object (c) Different expert synthesis intervals on LIBERO-Spatial.

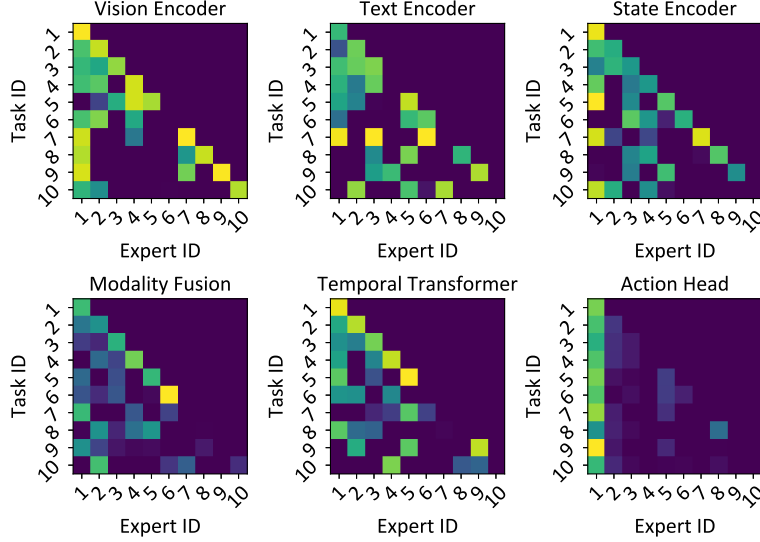


Figure 6: Visualization of expert coefficients on the LIBERO-Object benchmark.

replay (CR) ratio on overall performance. CR ratio refers to the proportion of router input-output pairs stored in the buffer for future replay. The results show that coefficient replay does not hinder forward transfer but helps mitigate forgetting efficiently, even when only a small fraction (e.g., 5%) of previous router input-output pairs is retained. Additionally, we demonstrate that replaying the context embeddings and coefficient vectors incurs a much lower storage overhead (approx. 6.7%) compared to replaying full expert demonstrations.

Computational Overhead. DMPEL introduces two additional computational stages: (1) encoding the current context with the frozen backbone and using the global router to compute routing coefficients, and (2) averaging the parameters of the top- δ experts to synthesize $\tilde{W} \in \mathbb{R}^{d_{in} \times d_{out}}$, which incurs approximately $2 \times \delta \times r \times (d_{in} + d_{out})$ FLOPs. Thereafter, the forward pass through the linear layer requires the usual $2 \times d_{in} \times d_{out}$ FLOPs. In robotic manipulation, which typically spans hundreds of decision steps and whose observations change only gradually from one step to the next, we conjecture that re-synthesizing policy parameters every several steps can yield a favorable trade-off between computational cost and task performance. Figure 5c verifies that, as the expert synthesis interval increases from 1 to 5, the average inference time rapidly approaches that of the backbone-only baseline (approx. 30 ms), while the success rate suffers only a slight decline. The result also indicates that the expert router indeed dynamically selects low-rank experts tailored to the current context.

Visualization on Expert Coefficients. We present a visualization of the expert coefficients for each sub-module during the lifelong learning process on the LIBERO-Object benchmark. As illustrated in Figure 6, significant knowledge sharing occurs across tasks, which contributes to the enhanced forward transfer capability of DMPEL. Notably, we observe that the low-rank expert learned for the

action head in the first task is extensively reused in subsequent tasks, while the experts introduced later are rarely activated. This suggests that these inactive experts can be pruned to further improve storage efficiency without adversely affecting performance.

6 Conclusion

In this study, we introduce Dynamic Mixture of Progressive Parameter-Efficient Expert Library (DMPEL) for lifelong robot learning. Our approach builds an low-rank expert library incrementally and utilizes a lightweight router to dynamically integrate these experts. This enables the robot to adapt flexibly to various scenarios over its lifetime. Additionally, by utilizing the modular nature of the policy, we address the issue of catastrophic forgetting through coefficient replay on the router, which allows for precise retrieval of experts on previous tasks. This method is significantly more efficient than the expensive demonstration replay on the entire policy. Our extensive experiments on the LIBERO benchmark show that DMPEL surpasses state-of-the-art lifelong learning baselines in terms of forward transfer and catastrophic forgetting while requiring only very few trainable parameters and storage.

Limitations. We conduct all experiments using a rather small model and we only use in-domain data to do pretraining and adaptation. We plan to further scale up our policy or employ more advanced VLA models (over billions of parameters) as the backbone in the future. In addition, we seek to further analyze the mechanisms of knowledge transfer and to enhance lifelong learning algorithms with a solid theoretical foundation.

References

- [1] Matthias De Lange, Rahaf Aljundi, Marc Masana, Sarah Parisot, Xu Jia, et al. A continual learning survey: Defying forgetting in classification tasks. *IEEE Transactions on Pattern Analysis and Machine Intelligence*, 44(7):3366–3385, 2021.
- [2] Gido M Van de Ven, Tinne Tuytelaars, and Andreas S Tolias. Three types of incremental learning. *Nature Machine Intelligence*, 4(12):1185–1197, 2022.
- [3] Marc Masana, Xialei Liu, Bartłomiej Twardowski, Mikel Menta, et al. Class-incremental learning: survey and performance evaluation on image classification. *IEEE Transactions on Pattern Analysis and Machine Intelligence*, 45(5):5513–5533, 2022.
- [4] Dhireesha Kudithipudi, Mario Aguilar-Simon, Jonathan Babb, Maxim Bazhenov, et al. Biological underpinnings for lifelong learning machines. *Nature Machine Intelligence*, 4(3):196–210, 2022.
- [5] Liyuan Wang, Xingxing Zhang, Hang Su, and Jun Zhu. A comprehensive survey of continual learning: theory, method and application. *IEEE Transactions on Pattern Analysis and Machine Intelligence*, 2024.
- [6] Jorge A Mendez and Eric Eaton. How to reuse and compose knowledge for a lifetime of tasks: A survey on continual learning and functional composition. *Transactions on Machine Learning Research*, 2023.
- [7] Anthony Brohan, Noah Brown, Justice Carbajal, Yevgen Chebotar, Joseph Dabis, et al. RT-1: Robotics transformer for real-world control at scale. *arXiv preprint arXiv:2212.06817*, 2022.
- [8] Anthony Brohan, Noah Brown, Justice Carbajal, Yevgen Chebotar, Xi Chen, et al. RT-2: Vision-language-action models transfer web knowledge to robotic control. *arXiv preprint arXiv:2307.15818*, 2023.
- [9] Scott Reed, Konrad Zolna, Emilio Parisotto, Sergio Gómez Colmenarejo, et al. A generalist agent. *Transactions on Machine Learning Research*, 2022.
- [10] Octo Model Team, Dibya Ghosh, Homer Walke, Karl Pertsch, Kevin Black, Oier Mees, Sudeep Dasari, Joey Hejna, Tobias Kreiman, Charles Xu, et al. Octo: An open-source generalist robot policy. *arXiv preprint arXiv:2405.12213*, 2024.

- [11] Moo Jin Kim, Karl Pertsch, Siddharth Karamcheti, Ted Xiao, Ashwin Balakrishna, Suraj Nair, Rafael Rafailov, Ethan P Foster, Pannag R Sanketi, Quan Vuong, et al. Openvla: An open-source vision-language-action model. In *8th Annual Conference on Robot Learning*.
- [12] Kevin Black, Noah Brown, Danny Driess, Adnan Esmail, Michael Equi, Chelsea Finn, Niccolo Fusai, Lachy Groom, Karol Hausman, Brian Ichter, et al. π_0 : A vision-language-action flow model for general robot control. *arXiv preprint arXiv:2410.24164*, 2024.
- [13] Rishi Bommasani, Drew A Hudson, Ehsan Adeli, Russ Altman, Simran Arora, Sydney von Arx, Michael S Bernstein, Jeannette Bohg, et al. On the opportunities and risks of foundation models. *arXiv preprint arXiv:2108.07258*, 2021.
- [14] Maxime Oquab, Timothée Darcet, Théo Moutakanni, Huy V. Vo, et al. DINOv2: Learning robust visual features without supervision. *Transactions on Machine Learning Research*, 2024.
- [15] Alec Radford, Jong Wook Kim, Chris Hallacy, et al. Learning transferable visual models from natural language supervision. In *International Conference on Machine Learning*, pages 8748–8763. PMLR, 2021.
- [16] Kaiming He, Haoqi Fan, et al. Momentum contrast for unsupervised visual representation learning. In *Proceedings of the IEEE/CVF Conference on Computer Vision and Pattern Recognition*, pages 9726–9735, 2020.
- [17] Kaiming He, Xinlei Chen, Saining Xie, et al. Masked autoencoders are scalable vision learners. In *Proceedings of the IEEE/CVF Conference on Computer Vision and Pattern Recognition*, pages 16000–16009, 2022.
- [18] Alexander Kirillov, Eric Mintun, Nikhila Ravi, Hanzi Mao, Chloe Rolland, et al. Segment anything. In *Proceedings of the IEEE/CVF International Conference on Computer Vision*, pages 4015–4026, 2023.
- [19] Tom Brown, Benjamin Mann, Nick Ryder, Melanie Subbiah, Jared D Kaplan, et al. Language models are few-shot learners. *Advances in Neural Information Processing Systems*, 33:1877–1901, 2020.
- [20] Hugo Touvron, Thibaut Lavril, Gautier Izacard, Xavier Martinet, Marie-Anne Lachaux, Timothée Lacroix, et al. Llama: Open and efficient foundation language models. *arXiv preprint arXiv:2302.13971*, 2023.
- [21] David Lopez-Paz and Marc’Aurelio Ranzato. Gradient episodic memory for continual learning. *Advances in Neural Information Processing Systems*, 30:6470–6479, 2017.
- [22] Arslan Chaudhry, Marcus Rohrbach, Mohamed Elhoseiny, et al. Continual learning with tiny episodic memories. *arXiv preprint arXiv:1902.10486*, 2019.
- [23] Hanul Shin, Jung Kwon Lee, Jaehong Kim, and Jiwon Kim. Continual learning with deep generative replay. *Advances in Neural Information Processing Systems*, 30:2994–3003, 2017.
- [24] Annie Xie and Chelsea Finn. Lifelong robotic reinforcement learning by retaining experiences. In *Conference on Lifelong Learning Agents*, pages 838–855. PMLR, 2022.
- [25] Jensen Gao, Annie Xie, Ted Xiao, Chelsea Finn, and Dorsa Sadigh. Efficient data collection for robotic manipulation via compositional generalization. *Proceedings of Robotics: Science and Systems (RSS)*, 2024.
- [26] Friedemann Zenke, Ben Poole, and Surya Ganguli. Continual learning through synaptic intelligence. In *International Conference on Machine Learning*, pages 3987–3995. PMLR, 2017.
- [27] James Kirkpatrick, Razvan Pascanu, Neil Rabinowitz, et al. Overcoming catastrophic forgetting in neural networks. *Proceedings of the National Academy of Sciences*, 114(13):3521–3526, 2017.
- [28] Zhizhong Li and Derek Hoiem. Learning without forgetting. *IEEE Transactions on Pattern Analysis and Machine Intelligence*, 40(12):2935–2947, 2017.

- [29] Andrei A Rusu, Neil C Rabinowitz, Guillaume Desjardins, Hubert Soyer, James Kirkpatrick, Koray Kavukcuoglu, Razvan Pascanu, and Raia Hadsell. Progressive neural networks. *arXiv preprint arXiv:1606.04671*, 2016.
- [30] Arun Mallya and Svetlana Lazebnik. Packnet: Adding multiple tasks to a single network by iterative pruning. In *Proceedings of the IEEE Conference on Computer Vision and Pattern Recognition*, pages 7765–7773, 2018.
- [31] Arun Mallya, Dillon Davis, and Svetlana Lazebnik. Piggyback: Adapting a single network to multiple tasks by learning to mask weights. In *European Conference on Computer Vision*, pages 67–82, 2018.
- [32] Ning Ding, Yujia Qin, Guang Yang, Fuchao Wei, Zonghan Yang, et al. Parameter-efficient fine-tuning of large-scale pre-trained language models. *Nature Machine Intelligence*, 5(3):220–235, 2023.
- [33] Junxian He, Chunting Zhou, Xuezhe Ma, Taylor Berg-Kirkpatrick, and Graham Neubig. Towards a unified view of parameter-efficient transfer learning. In *International Conference on Learning Representations*, 2021.
- [34] Neil Houlsby, Andrei Giurgiu, Stanislaw Jastrzebski, Bruna Morrone, et al. Parameter-efficient transfer learning for nlp. In *International Conference on Machine Learning*, pages 2790–2799. PMLR, 2019.
- [35] Shoufa Chen, Chongjian Ge, Zhan Tong, Jiangliu Wang, Yibing Song, Jue Wang, and Ping Luo. Adaptformer: Adapting vision transformers for scalable visual recognition. *Advances in Neural Information Processing Systems*, 35:16664–16678, 2022.
- [36] Edward J Hu, Phillip Wallis, Zeyuan Allen-Zhu, Yuanzhi Li, Shean Wang, Lu Wang, Weizhu Chen, et al. LoRA: Low-rank adaptation of large language models. In *International Conference on Learning Representations*, 2021.
- [37] Menglin Jia, Luming Tang, Bor-Chun Chen, Claire Cardie, Serge Belongie, Bharath Hariharan, and Ser-Nam Lim. Visual prompt tuning. In *European Conference on Computer Vision*, pages 709–727. Springer, 2022.
- [38] Xiang Lisa Li and Percy Liang. Prefix-tuning: Optimizing continuous prompts for generation. In *Proceedings of the 59th Annual Meeting of the Association for Computational Linguistics and the 11th International Joint Conference on Natural Language Processing (Volume 1: Long Papers)*, pages 4582–4597, 2021.
- [39] Brian Lester, Rami Al-Rfou, and Noah Constant. The power of scale for parameter-efficient prompt tuning. In *Proceedings of the 2021 Conference on Empirical Methods in Natural Language Processing*, pages 3045–3059, 2021.
- [40] Zuxin Liu, Jesse Zhang, Kavosh Asadi, Yao Liu, et al. TAIL: Task-specific adapters for imitation learning with large pretrained models. In *International Conference on Learning Representations*, 2024.
- [41] Thomas Schmied, Markus Hofmarcher, Fabian Paischer, Razvan Pascanu, and Sepp Hochreiter. Learning to modulate pre-trained models in rl. *Advances in Neural Information Processing Systems*, 36, 2023.
- [42] Daehee Lee, Minjong Yoo, Woo Kyung Kim, Wonje Choi, and Honguk Woo. Incremental learning of retrievable skills for efficient continual task adaptation. *Advances in Neural Information Processing Systems*, 37:17286–17312, 2024.
- [43] Bo Liu, Yifeng Zhu, Chongkai Gao, Yihao Feng, Qiang Liu, Yuke Zhu, and Peter Stone. Libero: Benchmarking knowledge transfer for lifelong robot learning. *Advances in Neural Information Processing Systems*, 36, 2024.
- [44] Roya Firoozi, Johnathan Tucker, Stephen Tian, Anirudha Majumdar, Jiankai Sun, Weiyu Liu, et al. Foundation models in robotics: Applications, challenges, and the future. *arXiv preprint arXiv:2312.07843*, 2023.

- [45] Yafei Hu, Quanting Xie, Vidhi Jain, Jonathan Francis, Jay Patrikar, Nikhil Keetha, et al. Toward general-purpose robots via foundation models: A survey and meta-analysis. *arXiv preprint arXiv:2312.08782*, 2023.
- [46] Simone Parisi, Aravind Rajeswaran, et al. The unsurprising effectiveness of pre-trained vision models for control. In *International Conference on Machine Learning*, pages 17359–17371. PMLR, 2022.
- [47] Zhecheng Yuan, Zhengrong Xue, Bo Yuan, et al. Pre-trained image encoder for generalizable visual reinforcement learning. *Advances in Neural Information Processing Systems*, 35:13022–13037, 2022.
- [48] Suraj Nair, Aravind Rajeswaran, Vikash Kumar, Chelsea Finn, and Abhinav Gupta. R3M: A universal visual representation for robot manipulation. In *Conference on Robot Learning*, pages 892–909. PMLR, 2023.
- [49] Ilija Radosavovic, Tete Xiao, Stephen James, Pieter Abbeel, Jitendra Malik, and Trevor Darrell. Real-world robot learning with masked visual pre-training. In *Conference on Robot Learning*, pages 416–426. PMLR, 2023.
- [50] Arjun Majumdar, Karmesh Yadav, Sergio Arnaud, Jason Ma, et al. Where are we in the search for an artificial visual cortex for embodied intelligence? *Advances in Neural Information Processing Systems*, 36, 2024.
- [51] Mohit Sharma, Claudio Fantacci, Yuxiang Zhou, et al. Lossless adaptation of pretrained vision models for robotic manipulation. In *International Conference on Learning Representations*, 2023.
- [52] Marcel Mittenbuehler, Ahmed Hendawy, Carlo D’Eramo, and Georgia Chalvatzaki. Parameter-efficient tuning of pretrained visual-language models in multitask robot learning. In *CoRL 2023 Workshop on Learning Effective Abstractions for Planning (LEAP)*, 2023.
- [53] Pierre Marza, Laetitia Matignon, Olivier Simonin, and Christian Wolf. Task-conditioned adaptation of visual features in multi-task policy learning. In *Proceedings of the IEEE/CVF Conference on Computer Vision and Pattern Recognition*, pages 17847–17856, 2024.
- [54] Anthony Liang, Ishika Singh, Karl Pertsch, and Jesse Thomason. Transformer adapters for robot learning. In *CoRL 2022 Workshop on Pre-training Robot Learning*, 2022.
- [55] Mengdi Xu, Yuchen Lu, Yikang Shen, Shun Zhang, Ding Zhao, and Chuang Gan. Hyper-decision transformer for efficient online policy adaptation. In *International Conference on Learning Representations*, 2023.
- [56] Yanyuan Qiao, Zheng Yu, and Qi Wu. Vln-petl: Parameter-efficient transfer learning for vision-and-language navigation. In *Proceedings of the IEEE/CVF International Conference on Computer Vision (ICCV)*, pages 15443–15452, October 2023.
- [57] Zifeng Wang, Zizhao Zhang, Chen-Yu Lee, Han Zhang, et al. Learning to prompt for continual learning. In *Proceedings of the IEEE/CVF Conference on Computer Vision and Pattern Recognition*, pages 139–149, 2022.
- [58] Zifeng Wang, Zizhao Zhang, Sayna Ebrahimi, et al. Dualprompt: Complementary prompting for rehearsal-free continual learning. In *European Conference on Computer Vision*, pages 631–648. Springer, 2022.
- [59] James Seale Smith, Leonid Karlinsky, Vyshnavi Gutta, et al. Coda-prompt: Continual decomposed attention-based prompting for rehearsal-free continual learning. In *Proceedings of the IEEE/CVF Conference on Computer Vision and Pattern Recognition*, pages 11909–11919, 2023.
- [60] Dahuin Jung, Dongyoon Han, Jihwan Bang, and Hwanjun Song. Generating instance-level prompts for rehearsal-free continual learning. In *Proceedings of the IEEE/CVF International Conference on Computer Vision*, pages 11847–11857, 2023.

- [61] Zhicheng Wang, Yufang Liu, Tao Ji, Xiaoling Wang, Yuanbin Wu, Congcong Jiang, Ye Chao, Zhencong Han, Ling Wang, Xu Shao, et al. Rehearsal-free continual language learning via efficient parameter isolation. In *Proceedings of the 61st Annual Meeting of the Association for Computational Linguistics (Volume 1: Long Papers)*, pages 10933–10946, 2023.
- [62] Anastasia Razdaibiedina, Yuning Mao, Rui Hou, Madian Khabisa, Mike Lewis, and Amjad Almahairi. Progressive prompts: Continual learning for language models. In *The Eleventh International Conference on Learning Representations*, 2023.
- [63] Dawei Zhou, Hailong Sun, et al. Continual learning with pre-trained models: A survey. *arXiv preprint arXiv:2401.16386*, 2024.
- [64] Qiankun Gao, Chen Zhao, Yifan Sun, Teng Xi, Gang Zhang, Bernard Ghanem, and Jian Zhang. A unified continual learning framework with general parameter-efficient tuning. In *Proceedings of the IEEE/CVF International Conference on Computer Vision*, pages 11483–11493, 2023.
- [65] Liyuan Wang, Jingyi Xie, Xingxing Zhang, Hang Su, and Jun Zhu. Hide-pet: continual learning via hierarchical decomposition of parameter-efficient tuning. *IEEE Transactions on Pattern Analysis and Machine Intelligence*, 2025.
- [66] Robert A Jacobs, Michael I Jordan, Steven J Nowlan, and Geoffrey E Hinton. Adaptive mixtures of local experts. *Neural computation*, 3(1):79–87, 1991.
- [67] William Fedus, Barret Zoph, and Noam Shazeer. Switch transformers: Scaling to trillion parameter models with simple and efficient sparsity. *Journal of Machine Learning Research*, 23(120):1–39, 2022.
- [68] Mohammed Muqeeth, Haokun Liu, and Colin Raffel. Soft merging of experts with adaptive routing. *Transactions on Machine Learning Research*, 2024.
- [69] Jonathan Frankle, Gintare Karolina Dziugaite, Daniel Roy, and Michael Carbin. Linear mode connectivity and the lottery ticket hypothesis. In *International Conference on Machine Learning*, pages 3259–3269. PMLR, 2020.
- [70] Gabriel Ilharco, Marco Tulio Ribeiro, Mitchell Wortsman, Ludwig Schmidt, Hannaneh Hajishirzi, and Ali Farhadi. Editing models with task arithmetic. In *The Eleventh International Conference on Learning Representations*, 2023.
- [71] Enneng Yang, Zhenyi Wang, Li Shen, Shiwei Liu, Guibing Guo, Xingwei Wang, and Dacheng Tao. Adamerging: Adaptive model merging for multi-task learning. In *The Twelfth International Conference on Learning Representations*, 2024.
- [72] Anke Tang, Li Shen, Yong Luo, Nan Yin, Lefei Zhang, and Dacheng Tao. Merging multi-task models via weight-ensembling mixture of experts. In *Proceedings of the 41st International Conference on Machine Learning*, pages 47778–47799, 2024.
- [73] Chengyue Wu, Teng Wang, Yixiao Ge, Zeyu Lu, Ruisong Zhou, Ying Shan, and Ping Luo. π -tuning: Transferring multimodal foundation models with optimal multi-task interpolation. In *International Conference on Machine Learning*, pages 37713–37727. PMLR, 2023.
- [74] Xun Wu, Shaohan Huang, and Furu Wei. Mixture of LoRA experts. In *International Conference on Learning Representations*, 2024.
- [75] Yaqing Wang, Sahaj Agarwal, Subhabrata Mukherjee, Xiaodong Liu, Jing Gao, Ahmed Hassan, and Jianfeng Gao. Adamix: Mixture-of-adaptations for parameter-efficient model tuning. In *Proceedings of the 2022 Conference on Empirical Methods in Natural Language Processing*, pages 5744–5760, 2022.
- [76] Weixiang Zhao, Shilong Wang, Yulin Hu, Yanyan Zhao, Bing Qin, Xuanyu Zhang, Qing Yang, Dongliang Xu, and Wanxiang Che. SAPT: A shared attention framework for parameter-efficient continual learning of large language models. In *Proceedings of the 62nd Annual Meeting of the Association for Computational Linguistics (Volume 1: Long Papers)*, pages 11641–11661, 2024.

- [77] Chengsong Huang, Qian Liu, Bill Yuchen Lin, Tianyu Pang, Chao Du, and Min Lin. Lorahub: Efficient cross-task generalization via dynamic lora composition. In *First Conference on Language Modeling*, 2024.
- [78] Jonas Pfeiffer, Aishwarya Kamath, Andreas Rücklé, Kyunghyun Cho, and Iryna Gurevych. Adapterfusion: Non-destructive task composition for transfer learning. In *Proceedings of the 16th Conference of the European Chapter of the Association for Computational Linguistics: Main Volume*, pages 487–503, 2021.
- [79] Viraj Shah, Nataniel Ruiz, Forrester Cole, Erika Lu, Svetlana Lazebnik, Yuanzhen Li, and Varun Jampani. Ziplora: Any subject in any style by effectively merging loras. In *European Conference on Computer Vision*, pages 422–438. Springer, 2024.
- [80] Donald Shenaj, Ondrej Bohdal, Mete Ozay, Pietro Zanuttigh, and Umberto Michieli. Lora.rar: Learning to merge loras via hypernetworks for subject-style conditioned image generation. *arXiv preprint arXiv:2412.05148*, 2024.
- [81] Yang Yang, Wen Wang, Liang Peng, Chaotian Song, Yao Chen, Hengjia Li, Xiaolong Yang, Qinglin Lu, Deng Cai, Boxi Wu, et al. Lora-composer: Leveraging low-rank adaptation for multi-concept customization in training-free diffusion models. *arXiv preprint arXiv:2403.11627*, 2024.
- [82] Chuanyu Yang, Kai Yuan, Qiuguo Zhu, Wanming Yu, and Zhibin Li. Multi-expert learning of adaptive legged locomotion. *Science Robotics*, 5(49):eabb2174, 2020.
- [83] Runhan Huang, Shaoting Zhu, Yilun Du, and Hang Zhao. MoE-LoCo: Mixture of experts for multitask locomotion. *arXiv preprint arXiv:2503.08564*, 2025.
- [84] Han Zhao, Wenxuan Song, Donglin Wang, Xinyang Tong, Pengxiang Ding, Xuelian Cheng, and Zongyuan Ge. More: Unlocking scalability in reinforcement learning for quadruped vision-language-action models. *arXiv preprint arXiv:2503.08007*, 2025.
- [85] Yixiao Wang, Yifei Zhang, Mingxiao Huo, Thomas Tian, Xiang Zhang, Yichen Xie, Chenfeng Xu, Pengliang Ji, Wei Zhan, Mingyu Ding, et al. Sparse diffusion policy: A sparse, reusable, and flexible policy for robot learning. In *8th Annual Conference on Robot Learning*, 2024.
- [86] Michael Bain and Claude Sammut. A framework for behavioural cloning. In *Machine Intelligence 15*, pages 103–129, 1995.
- [87] Natalia Díaz Rodríguez, Vincenzo Lomonaco, David Filliat, and Davide Maltoni. Don’t forget, there is more than forgetting: new metrics for continual learning. *arXiv preprint arXiv:1810.13166*, 2018.
- [88] Huang Huang, Fangchen Liu, Letian Fu, Tingfan Wu, Mustafa Mukadam, Jitendra Malik, Ken Goldberg, and Pieter Abbeel. Otter: A vision-language-action model with text-aware visual feature extraction. *arXiv preprint arXiv:2503.03734*, 2025.
- [89] Ethan Perez, Florian Strub, Harm De Vries, Vincent Dumoulin, and Aaron Courville. Film: Visual reasoning with a general conditioning layer. In *Proceedings of the AAAI conference on artificial intelligence*, volume 32, 2018.
- [90] Yichen Wu, Hongming Piao, Long-Kai Huang, Renzhen Wang, Wanhua Li, Hanspeter Pfister, Deyu Meng, Kede Ma, and Ying Wei. Sd-lora: Scalable decoupled low-rank adaptation for class incremental learning. In *The Thirteenth International Conference on Learning Representations*, 2025.
- [91] Xiao Wang, Tianze Chen, Qiming Ge, Han Xia, Rong Bao, Rui Zheng, Qi Zhang, Tao Gui, and Xuanjing Huang. Orthogonal subspace learning for language model continual learning. In *The 2023 Conference on Empirical Methods in Natural Language Processing*.
- [92] Weikang Wan, Yifeng Zhu, Rutav Shah, and Yuke Zhu. Lotus: Continual imitation learning for robot manipulation through unsupervised skill discovery. In *2024 IEEE International Conference on Robotics and Automation (ICRA)*, pages 537–544. IEEE, 2024.

A Experimental Details

A.1 Policy and Algorithm Details

As illustrated in Section 4.1, we use an auto-regressive policy consisting of vision, text, and state encoders, an input modality fusion module, a temporal transformer, and an action head [40, 43]. Detailed hyperparameters of each submodule are summarized in Table 1.

We utilize the implementations of Experience Replay (ER) [22], Elastic Weight Consolidation (EWC) [27], and PackNet [30] as provided in LIBERO [43]. For ER, we employ a replay ratio of 20%. For EWC, we set the hyperparameters $\gamma = 0.9$ and $\lambda = 5 \times 10^4$. For PackNet, we fix 25% of the parameters as important. When training with ER and EWC, we use two GPUs, each with a batch size of 16, ensuring the total batch size remains consistent with other methods. For additional details on these baselines, we refer readers to [43]. We directly use the official code of LOTUS [92]. Since LOTUS employs a distinct architecture, we adjust its parameters to be comparable to our policy and follow the same training pipeline. Additionally, LOTUS utilizes the DINO-v2 [14] foundation model instead of CLIP, as recommended by the ablation study in their paper.

For LoRA-based methods, we insert LoRA modules with rank $r = 8$ into the 6-th to 11-th layers of the CLIP image and text encoders, and LoRA modules with $r = 16$ into the temporal transformer. LoRA is applied to the query and value projection matrices. In TAIL and IsCiL, we learn task-specific fusion modules, state encoders, and action heads, as described in [40]. In contrast, these components are frozen in L2M following the original paper [41]. Due to the unavailability of publicly released code for TAIL, we implemented it based on the description in the paper [40]. We integrated the code for L2M and IsCiL into our codebase, as the original implementations operate with different policies across different benchmarks. For L2M, we use a pool size of 30 and the similarity loss coefficient $\lambda = 0.5$. For IsCiL, we set the skill prototype \mathcal{X}_z in \mathcal{X} to be composed of 20 bases as in [42]. For DMPEL, we adopt the same LoRA settings in the image encoder, text encoder, and temporal transformer, and use LoRA experts with $r = 16$ for all linear layers in other submodules. Besides, in the Long suite, we tune both the low-rank weights \mathbf{A}, \mathbf{B} and biases \mathbf{b} , whereas in the Goal, Spatial, and Object suites, we only tune the low-rank weights \mathbf{A}, \mathbf{B} . However, both settings lead to fewer learnable parameters than TAIL [40], which learns these sub-modules separately for each task. We also employ dropout with probability $p = 0.15$ on the coefficient for low-rank experts to avoid overfitting.

Table 1: Environment and Policy Architecture Configuration

Hyperparameter	Value	Hyperparameter	Value
<i>Vision & Text Encoder</i>			
Pretrained model	CLIP ViT-B/16 [15]	Image resolution	128*128
<i>Proprioceptive States</i>			
Joint state dim.	7	Gripper state dim.	2
<i>Modality Fusion</i>			
Number of hidden layers	1	Hidden size	256
Activation	GELU		
<i>Temporal Transformer</i>			
Number of layers	6	Number of attn. heads	8
Embedding size	768	MLP hidden size	1024
Max sequence Length	10	Dropout	0.15
<i>Action Head</i>			
Number of hidden layers	2	Hidden size	256
Number of Modes	5	Min. std	1e-4
Activation	Softplus	Action dim.	7
<i>Expert router</i>			
Number of hidden layers	2	Hidden Activation	GELU
Output Activation	Sigmoid		

A.2 Training Configuration

We generally follow the setup in the LIBERO benchmark for training and evaluation [43]. Detailed settings and hyperparameters are summarized in Table 2. For all experiments, we use either Nvidia A100 or H800 GPUs. We employ Distributed Data Parallel (DDP) for parallel training across 4 GPUs during pretraining, while using a single GPU for lifelong learning. We utilize the 16-bit floating point precision (FP16) training mode to accelerate the training process. To ensure reproducibility, we adopted three random seeds, 100, 200, 300, and we report the mean and standard deviation of the performance over three seeds throughout the paper.

Table 2: Training Hyperparameters

Hyperparameter	Value	Hyperparameter	Value	Hyperparameter	Value
<i>Optimizer</i>					
Training epochs	10	Batch size	32	Optimizer	AdamW
Betas	(0.9,0.999)	Learning rate	1e-4	Anneal strategy	cos
Weight decay	0.1	Gradient clip	100		
<i>Image Augmentation</i>					
Brightness	0.3	Saturation	0.3	Contrast	0.3
Hue	0.3	Color jitter prob.	0.9	Rotation	15
Translation	0.1	Affine prob.	0.6		
<i>Evaluation</i>					
Epochs per eval.	2	Eval. episodes	20		

A.3 Benchmark Details

We present the language instructions for the tasks in four lifelong learning LIBERO task suites in Table 3. Although some tasks have similar descriptions, they are not identical due to differences in environment configurations, such as varying spatial layouts, objects, or goal positions. Each task provides 50 successful expert demonstrations for imitation learning.

B Additional Results

B.1 Learning curves

We present the learning curves for all methods in four lifelong learning LIBERO task suites in Figure 7-10. The y -axis indicates the success rate, while the x -axis depicts the agent’s training process over the course of lifelong learning. For example, the Task 1 subplot in the figure shows the agent’s performance on the first task as it learns ten tasks sequentially.

Table 3: Taks Instructions of LIBERO Task Suites

Suite	Instructions
Goal	open the middle drawer of the cabinet put the bowl on the stove put the wine bottle on top of the cabinet open the top drawer and put the bowl inside put the bowl on top of the cabinet push the plate to the front of the stove put the cream cheese in the bowl turn on the stove put the bowl on the plate put the wine bottle on the rack
Spatial	pick up the black bowl between the plate and the ramekin and place it on the plate pick up the black bowl next to the ramekin and place it on the plate pick up the black bowl from table center and place it on the plate pick up the black bowl on the cookie box and place it on the plate pick up the black bowl in the top drawer of the wooden cabinet and place it on the plate pick up the black bowl on the ramekin and place it on the plate pick up the black bowl next to the cookie box and place it on the plate pick up the black bowl on the stove and place it on the plate pick up the black bowl next to the plate and place it on the plate pick up the black bowl on the wooden cabinet and place it on the plate
Object	pick up the alphabet soup and place it in the basket pick up the cream cheese and place it in the basket pick up the salad dressing and place it in the basket pick up the bbq sauce and place it in the basket pick up the ketchup and place it in the basket pick up the tomato sauce and place it in the basket pick up the butter and place it in the basket pick up the milk and place it in the basket pick up the chocolate pudding and place it in the basket pick up the orange juice and place it in the basket
Long	put both the alphabet soup and the tomato sauce in the basket put both the cream cheese box and the butter in the basket turn on the stove and put the moka pot on it put the black bowl in the bottom drawer of the cabinet and close it put the white mug on the left plate and put the yellow and white mug on the right plate pick up the book and place it in the back compartment of the caddy put the white mug on the plate and put the chocolate pudding to the right of the plate put both the alphabet soup and the cream cheese box in the basket put both moka pots on the stove put the yellow and white mug in the microwave and close it

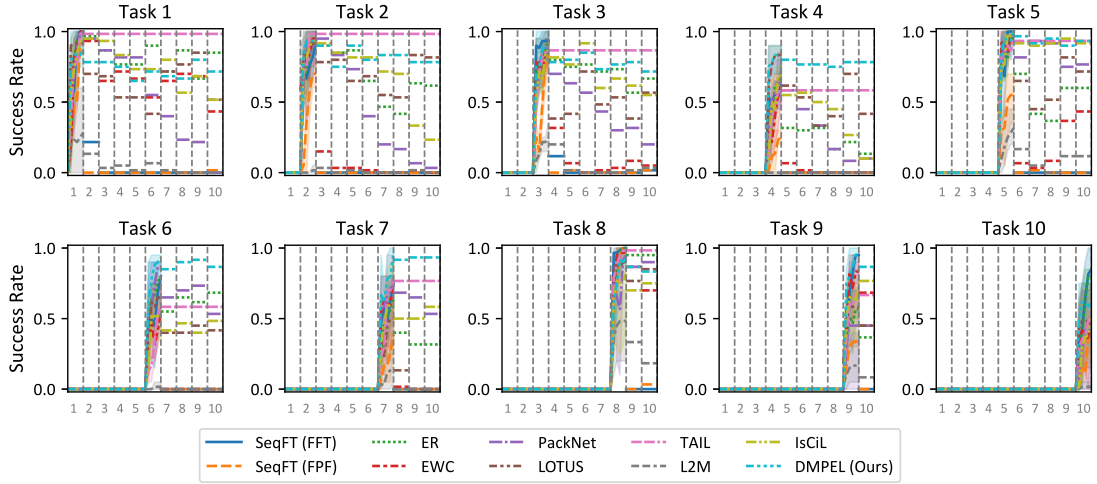


Figure 7: Visualization of learning curves on the LIBERO-Goal benchmark.

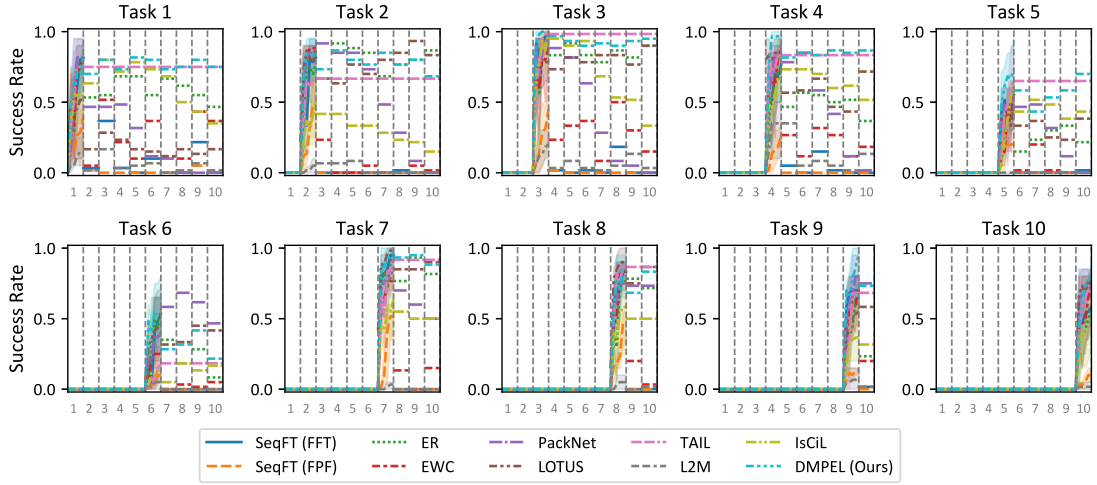


Figure 8: Visualization of learning curves on the LIBERO-Spatial benchmark.

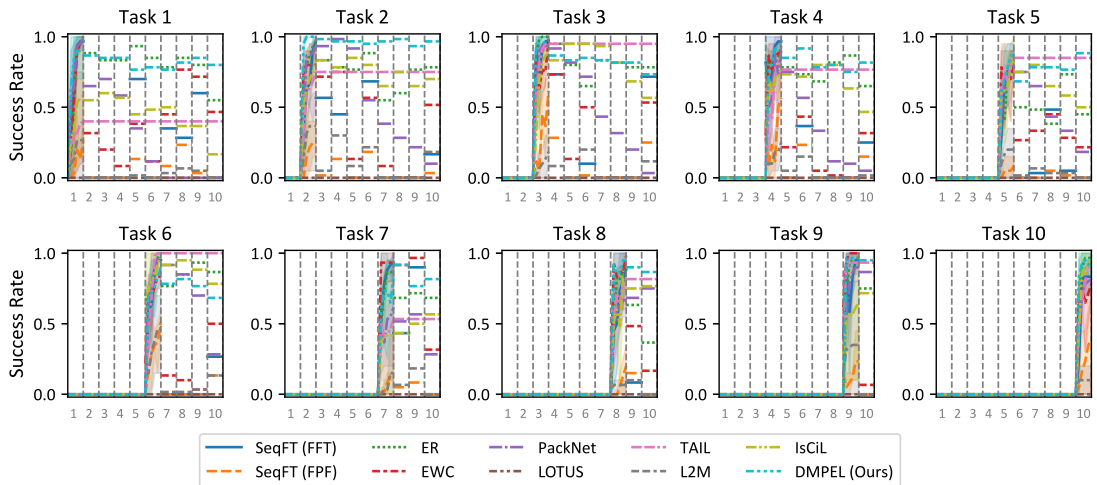


Figure 9: Visualization of learning curves on the LIBERO-Object benchmark.

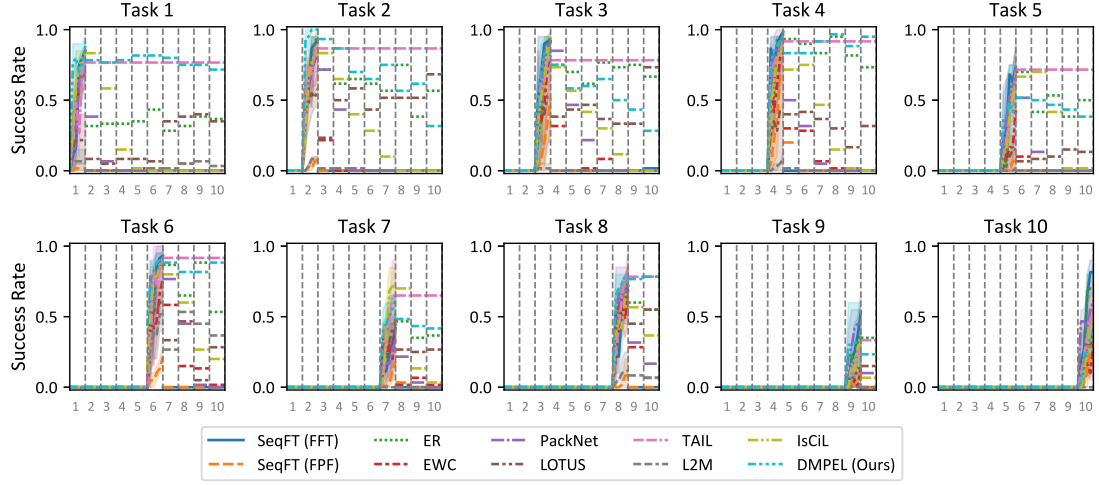


Figure 10: Visualization of learning curves on the LIBERO-Long benchmark.